IOP Publishing Journal of Micromechanics and Microengineering

J. Micromech. Microeng. **17** (2007) 1533–1541 doi:10.1088/0960-1317/17/8/016

# Fabrication of round channels using the surface tension of PDMS and its application to a 3D serpentine mixer

**Kangsun Lee[1,2], Choong Kim[2], Kyeong Sik Shin[2], Jin Woo Lee[3], Byeong-Kwon Ju[3], Tae Song Kim[2], Seung-Ki Lee[1] and Ji Yoon Kang[2]**

[1] MEMS Laboratory, School of Electrical, Electronic & Computer Engineering, Dankook University, Seoul, Republic of Korea
[2] Nano-Bio Research Center, Korea Institute of Science and Technology, Seoul, Republic of Korea
[3] Display and Nanosystem Laboratory, College of Engineering, Korea University, Republic of Korea

Received 8 January 2007, in final form 29 May 2007
Published 5 July 2007
Online at stacks.iop.org/JMM/17/1533

**Abstract**
A novel fabrication technique was developed to fabricate round microchannels and applied to a micro mixer having a barrier structure using surface tension of PDMS. When the solidified PDMS layer (channel layer) contacts the liquid PDMS film (meniscus layer), a meniscus is formed around the sidewall in the microchannel due to surface tension. The external load pressure and contact area of the channel layer were adjusted to form various cross-sectional shapes such as a U shape, ellipse, semi-circle and circle. Since the width of the channel also determines the depth formed by the difference in capillary height, a multi-depth channel can be fabricated using a one-step process. It was applied to a dual-depth serpentine mixer, eliminating the aligned bonding of conventional soft lithography. The 3D-structure mixer enhanced mixing performance in the range of $Re > 10$ compared with a 2D-structure. It could fully mix phenolphthalein and sodium hydroxide when the Reynolds number was 80. The suggested fabrication method could be very useful in various microfluidic devices that need round corners and multi-depth channels.

(Some figures in this article are in colour only in the electronic version)

## 1. Introduction

MEMS (micro electro mechanical system) technology has enabled the commercialization of tiny electrical devices including pressure sensors, accelerometers and micro display mirrors. Its application area is expanding to biochemical applications. Like the integrated circuit in electronics, the microfluidic circuit is expected to automate biological and chemical analysis with high density and throughput. Hence, many research groups are paying attention to various kinds of biochips for the analysis of DNA, protein and cell, since the lab-on-a-chip (LOC) can effectively handle a small volume of liquid and also decrease laborious work and experimental error.

Glass is a popular substrate of microfluidic chips because of its robust surface stability and high dielectric constant, but it is not widely used in research because of its high cost and long process time. For rapid prototyping of the test design, soft-lithography using PDMS (polydimethylsiloxane) is preferable and widely used by chemists and biologists [1]. However, the cross-section of the PDMS microchannel is usually limited to a rectangular shape since the mold is a thick photoresist like SU-8 or silicon etched by a deep reactive ion etcher. Hence, alternative mold fabrication methods including solid printing [2] and gray scale photolithography [3] were reported to adapt various applications of microfluidic chip. A channel with bell-shaped cross-section was fabricated with UV light diffraction

  

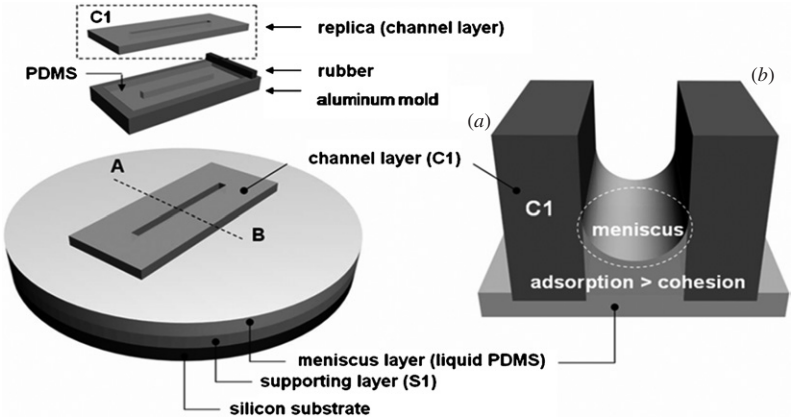


**Figure 1.** Principle of microchannel fabrication having a round cross-section using surface tension.

[4] for better leak-proof performance of the membrane valve [5]. In addition to valve application, a round channel is also advantageous in mimicking the human vein. When a vascular structure is needed in tissue scaffolding, the round microfluidic channel is considered as a good candidate for an artificial capillary vessel. The circular cross-section is suitable for imitating natural veins since the diffusion of nutrition and gases from a circular channel is most uniform. Another merit of a round channel is that no stagnation occurs at the corner edges when the microfluidic chip is subjected to a separation process such as liquid chromatography. The stagnation of flow, which occurs at the corners of a rectangular channel, is not observed in a circular channel owing to the perfectly symmetrical velocity profile [6]. A round channel induces no retardation in the corner region that leads to tailing of the analyte plug, which increases the plate number of separation.

Therefore, this paper suggests a novel fabrication method for a round channel using surface tension. The meniscus of liquid PDMS in the capillary is utilized to create a round channel. When solid PDMS with an open vertical channel squeezes down the spin-coated liquid PDMS, the surface tension of the sidewall pulls up the liquid and forms a round meniscus. This method is able to make several cross-sections of a circle or ellipse as well as semi-circle or U shape having different depths with one mask process. In addition, this fabrication method does not need a bonding process, since liquid PDMS plays a role in the adhesive bonding layer [7, 8]. We applied the suggested method to the fabrication of a three-dimensional (3D) serpentine mixer [9] as one of the most efficient mixers ever reported [10–12]. The suggested method eliminates the cumbersome precise aligned bonding of microchannel layers to create a 3D structure and realize a dual height microfluidic channel with just one mask. The characteristics of fabrication for a round microchannel and the performance of the serpentine 3D micro mixer fabricated by the surface tension of PDMS with one mask are analyzed and discussed.

## 2. A round microchannel using surface tension

### *2.1. The meniscus of liquid PDMS at the channel*

We fabricated a micro channel of round cross-section using the surface tension between liquid PDMS and solid PDMS sidewalls [13–15]. The aluminum mold was precisely machined (surface roughness of 3 $\mu$m) to form a protruded thin rectangle with 500 $\mu$m width and 1000 $\mu$m thickness. After liquid PDMS was poured into the mold, it was wiped out with a rubber bar as depicted in figure 1. The PDMS was cured and peeled off to obtain the open channel layer (C1). The liquid PDMS layer with 30 $\mu$m thickness (meniscus layer) was spin-coated on the cured PDMS slab (supporting layer, S1). The supporting layer's thickness was 500 $\mu$m (S1), which was previously coated and cured on the silicon wafer. When the PDMS channel layer (C1) was placed on the meniscus layer and pressed against it, liquid PDMS was squeezed in the inside of the channel and formed a meniscus due to surface tension. The contact angle at the meniscus was around 20° since the adhesion force between the liquid PDMS and sidewall PDMS is bigger than the molecular forces of liquid PDMS. This phenomenon allows us to make various cross-sectional shapes such as a semi-circle or ellipse by adjusting the film thickness of the liquid PMDS, the channel width, external load pressure, and contact area of the channel layer (C1) on the liquid PDMS film.

### *2.2. Fabrication of PDMS round the channel*

The meniscus of liquid PDMS was used to fabricate a microchannel with circular cross-section as depicted in figure 2(*a*).

(1) The channel layer (C1) with an open rectangular channel was fabricated by aluminum mold.
(2) The liquid PDMS was coated on the silicon wafer for 20 s at a speed of 300 rpm in a spin-coater and baked for 5 min at 100 °C in a hot plate to create a supporting layer of 500 $\mu$m thickness (S1).
(3) The liquid PDMS film was coated on the supporting layer (S1) for 1 min at a speed of 2000 rpm by a spin-coater to make a meniscus layer and the thickness was 30 $\mu$m.
(4) The channel layer (C1) was placed on the top of the meniscus layer, and the channel layer (C1) was uniformly pressed down by loading weight (50–500 g). At that time, the liquid PDMS formed a meniscus inside the channel.
(5) The upper layer (C1+meniscus layer+S1) was baked for 5 min at 100 °C and was separated from the silicon substrate.

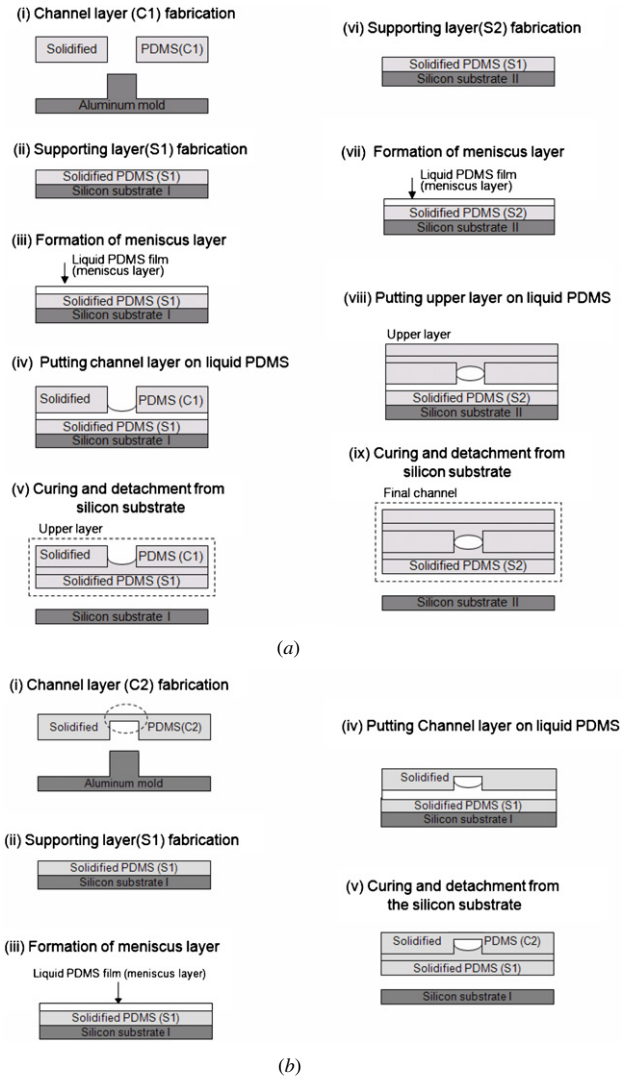


**Figure 2.** Fabrication process of the microchannel for (*a*) a circular cross-section and (*b*) a semi-circular cross-section.

(6) The liquid PDMS was coated on another silicon substrate and baked for 5 min at 100 °C to make another supporting layer of 500 $\mu$m thickness (S2).
(7) The liquid PDMS film was coated for 1 min at a speed of 2000 rpm by a spin-coater to make a meniscus layer of 30 $\mu$m thickness.
(8) The upper layer (C1+meniscus layer+S1) was placed on the top of another meniscus layer. At that time, the liquid PDMS formed another meniscus inside the channel.
(9) The whole layer (upper layer+meniscus layer+S2) was baked for 5 min at 100°C and was separated from the silicon substrate.

This method can also fabricate a semi-circle cross-section as presented in figure 2(*b*). Most of the processes are similar to the previous fabrication method except that the channel layer (C2) has a concave and closed channel. When the layer (C2) was placed on the meniscus layer, the PDMS was extruded into the C2 layer channel and the meniscus was formed. When the upper layer (C2+meniscus layer+S1) was cured and separated from the silicon substrate, a microchannel with semi-circle cross-section was obtained.

### *2.3. The effect of external load pressure on the channel shape*

The geometric variables of the meniscus are described in figure 3, where $h_1$ is the meniscus height induced by the surface tension of the sidewall in a solid open channel layer (C1), $R$ is the radius of the meniscus and $\theta$ is the contact angle of liquid PDMS. The shape of the meniscus is described by $h_0$, $h_1$ and $w_1$, which are the height of the liquid PDMS extruded through the opening of the solid PDMS (C1), the length of the meniscus and the width of the flat surface between the two menisci, respectively. $P$ is the load weight, $t_0$ is the initial thickness of the liquid PDMS after deposition and $t_1$ is the final thickness of the liquid PDMS after contact of the C1 layer.

The width of channel determines the length of the flat area ($w_1$) due to gravity. The length of the meniscus is characterized by capillary length $\kappa^{-1}$, beyond which gravity becomes important:

$$\kappa^{-1} = \sqrt{\gamma/\rho g}, \tag{1}$$

where $\rho$ is the density of the PDMS, $g$ is the acceleration of gravity and $\gamma$ is the surface tension of the PDMS in air. The capillary length of the PDMS is around 1.5 mm [16]. When $w$ is larger than $\kappa^{-1}$, the channel has a flat area due to gravity and is a rectangle with four round corners. Because the channel width considered in this paper does not exceed 1 mm, the rectangular cross-section cannot be formed. Hence, we only considered the case without a flat area, $w_1 = 0$.

The controllable parameters for the cross-section shape are the load weight ($P$) and the width of the mold ($w_{\mathrm{mod}}$). In the characterization of the effect of load weight, the width of the slit was fixed as 500 $\mu$m and the initial thickness of the liquid PDMS film was 30 $\mu$m. We investigated the effect of the pressing load on the rising height of the PDMS and meniscus shape. After curing, we measured the rising height of the PDMS after pressing ($h_0$) and the height ($h_1$) and contact angle ($\theta$) of the meniscus as a function of the load weight. The load weight was changed from 50 g to 500 g and the rising height, $h_0$, was plotted in figure 4(*a*). The mass load of the solidified PDMS (C1) can also be another variable for the load, but the mass load is negligible when compared with that of the external load. As the weight increased, it was observed that the height $h_0$ increased from 50 $\mu$m to 700 $\mu$m. Though the final thickness of the PDMS liquid layer $t_1$ could not be measured due to the unclear boundary of the cured PDMS, it must be decreased by loading weight. Rising height was determined by the squeezed volume and it was proportional to the load weight [17]. However, the generalized squeeze flow equation (2) is inadequate to estimate the rising height since the viscosity of the PDMS is time-varying due to the curing of the PDMS at room temperature:

$$\frac{\mathrm{d}h_0(t)}{\mathrm{d}t} = P_L \frac{h_0^3(t)}{6\mu(t)} \frac{1}{w_{\mathrm{mold}} w} \tag{2}$$

where $P_L$ is the loading pressure, $\mu$ is the viscosity of the PDMS, $w_{\mathrm{mold}}$ is the width of the mold and $w$ is the channel width. We can roughly guess the approximate solution but the highly nonlinear term in Reynold's equation might cause serious errors in the real experiment. Nevertheless, $h_0$ can be controlled by the experiment since the squeezed flow speed through the thin film layer is very slow, in the order of a few

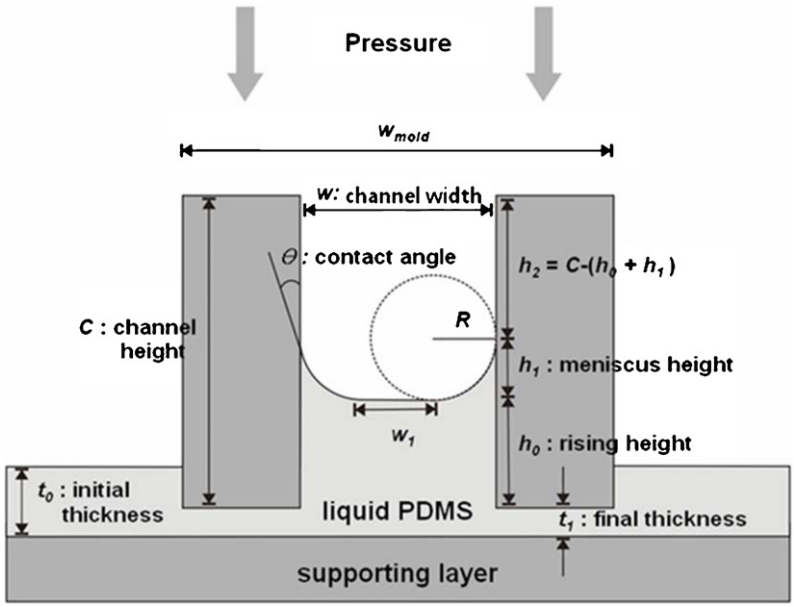


**Figure 3.** Parameters and variables for fabrication of the microchannel having a round cross-section using external load pressure.

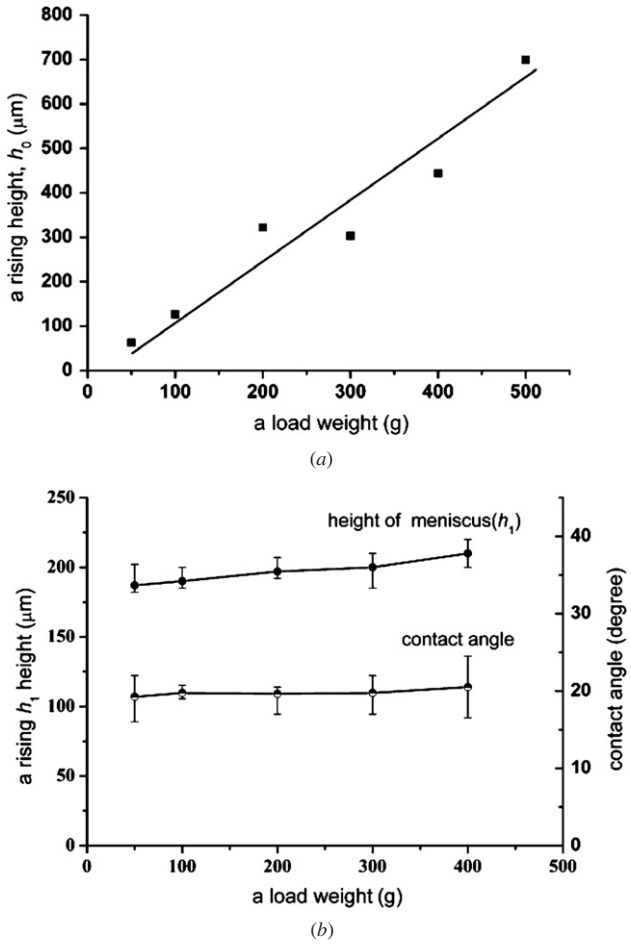


**Figure 4.** (*a*) The plot of rising height, $h_0$ and (*b*) the height of meniscus, $h_1$ and contact angle as a function of load weight.

$\mu$m per min. When the load is enough to fully squeeze out the volume of the 30 $\mu$m thick PDMS layer, we can calculate the

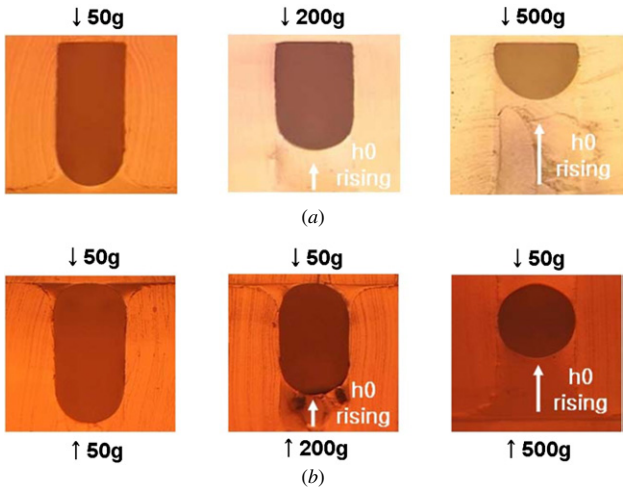


**Figure 5.** Microscope image of the cross-section of the fabricated microchannel: (*a*) processed only in one side in liquid PDMS (one-stacking process) and (*b*) processed in all sides in liquid PDMS (double-stacking process).

rising height by the squeezed volume. The extruded height $h_0$ is expressed as in equation (3) since the squeezed volume must be equal to the rising volume in an open vertical channel,

$$h_0 = \frac{w_{\text{mold}}}{w}(t_0 - t_1) \equiv \frac{w_{\text{mold}}}{w} t_{\text{sq}}, \tag{3}$$

where $t_{\text{sq}}$ is the squeezed thickness of the liquid PDMS. As the width of the solid PDMS layer ($w_{\text{mold}}$) is 16 mm and $t_{\text{sq}}$ is 30 $\mu$m, the rising height $h_0$ is about 720 $\mu$m. The calculated height is well matched to the case of 500 g load, which means 500 g is enough to squeeze out almost all the liquid PDMS layer. The experimental error resulted from the manual handling of the load, which causes the S1 layer not to be parallel enough to produce reliable squeezing. If equipment with precise parallel alignment were used, the height could be

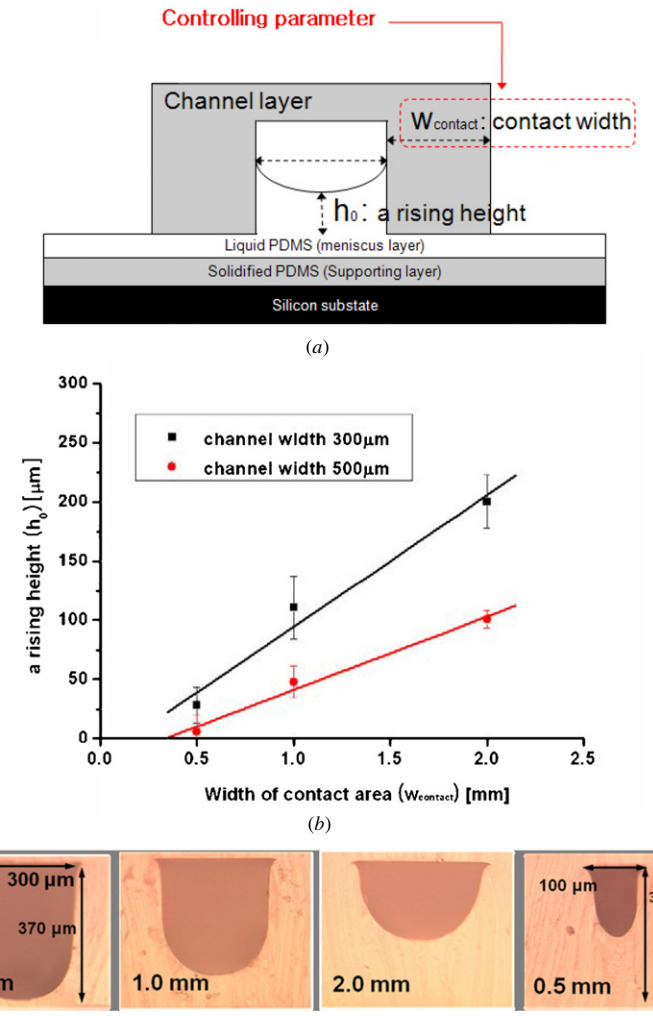


**Figure 6.** (*a*) Parameters and variables for fabrication of the microchannel having a round cross-section controlling the contact areas, (*b*) plot of rising height, $h_0$, as a function of contact width ($w_{\text{contact}}$), (*c*) images of the cross-section in the microchannel of 300 $\mu$m size by adjusting the width of the contact area and cross-sectional image of the microchannel of 100 $\mu$m width (right).

controlled with ease. Figure 4(*b*) shows that the contact angle and meniscus height were nearly constant at all load pressures since the meniscus depends on only the surface tension of the liquid PDMS.

Several shapes of cross-sections were fabricated including a semi-circle, circle, ellipse and 'U' shaped round channel by adjusting the load weight. Figure 5(*a*) shows the cross-sectional shape of the channels fabricated by the one-side stacking process of channel layer. The more the load weight is increased, the higher is the rising height of the PDMS ($h_0$). Hence, the cross-section was changed from a 'U' shape cross-section to a semi-circle one. Figure 5(*b*) represents the channels from the double-side stacking process. We were able to fabricate various cross-sections including an ellipse and circle by increasing the load weight. Manual manipulation of the load weight made it difficult to control the exact rising height of the PDMS ($h_0$); however, the meniscus height and the contact angle were almost constant. Therefore, we anticipate that this fabrication method can be improved if we use a precise machine for the load pressure or a vacuum chamber.

### *2.4. The effect of mold contact area on the channel shape*

To make a smaller round channel of less than 500 $\mu$m, we should exactly control the amount of liquid PDMS squeezed into a microchannel. However, it was not easy to control the amount of liquid PDMS squeezed by the large mold contact area pressed by the external loading pressure. The amount of the squeezed liquid PMDS was excessive and they fully filled the inside of the microchannel. To make a round microchannel of a smaller size, the contact area of the channel layer should be adjusted as shown figure 6(*a*). So, we investigated the relation between the contact area and the amount of squeezed liquid PDMS. To characterize the relation, we fabricated PDMS microchannels where the height was 360 $\mu$m and the width was 300 $\mu$m and 500 $\mu$m, respectively, using soft-lithography. At that time, the contact areas of each microchannel were adjusted to 0.5 mm, 1.0 mm and 2.0 mm, respectively. Figure 6(*b*) shows that the larger the contact area, the higher the rising height. The height was almost linearly proportional to the contact areas. Also, we could observe that the rising height was increased when the channel width was decreased.

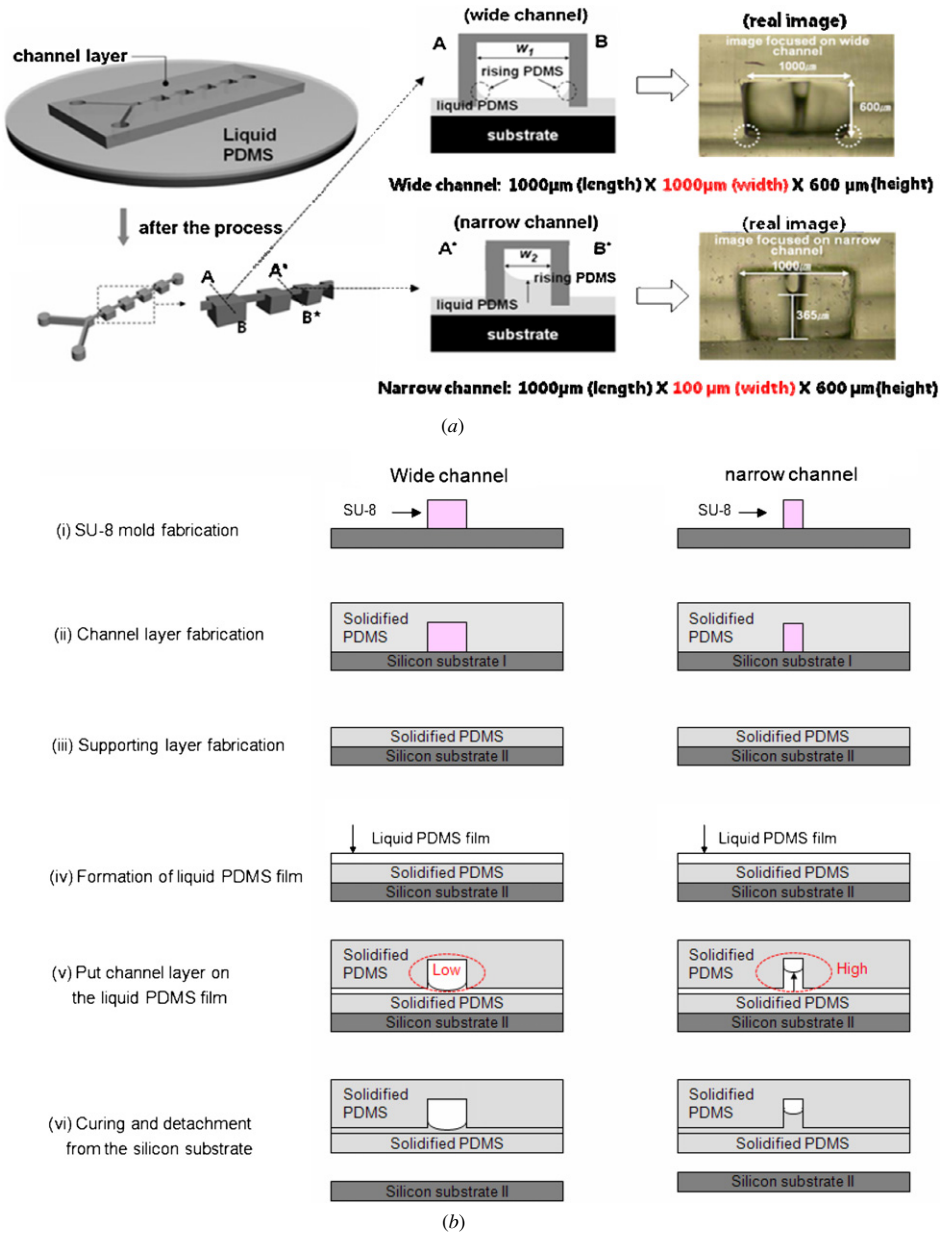


**Figure 7.** (*a*) Barrier structured microchannel images using surface tension by varying the microchannel width, (*b*) fabrication process of a mixer with barriers; the right is process flow focused on a wide channel, and the left is process flow focused on a narrow channel.

Figure 6(*c*) shows cross-section images of a 300 $\mu$m channel when the contact areas were adjusted. A 100 $\mu$m channel was also tried by this method; however, the squeezed volume of 30 $\mu$m PDMS film exceeds the capacity of the channel when the contact area was 1 mm and 2 mm except 0.5 mm. This experimental result implied that a smaller channel can be fabricated by adjusting the contact area, and also that the minimum size of a round channel is limited by the thickness of the squeezed PDMS film.

## 3. Micro mixer using the surface tension of PDMS

The capillary effect of PDMS could make a circular channel using round meniscus at the side wall, and the width of the channel was considered as a control parameter of rising height. In this section, the width of the channel was controlled to create a three-dimensional micro mixer with dual depth.

### *3.1. Principle and fabrication method*

The rising height of the round channel in equation (3) is a function of channel width. Since the height is inversely proportional to the width of the channel, a wide channel has a deeper channel than a narrow channel at a given load. This property can make a multi-depth microchannel in PDMS with one mask. It was applied to a 3D serpentine mixer having different depths. Figure 7(*a*) represents a schematic diagram of the fabrication method to make a micro mixer with the barrier structure implemented by varying the channel height. When the channel layer with connected narrow and wide channels

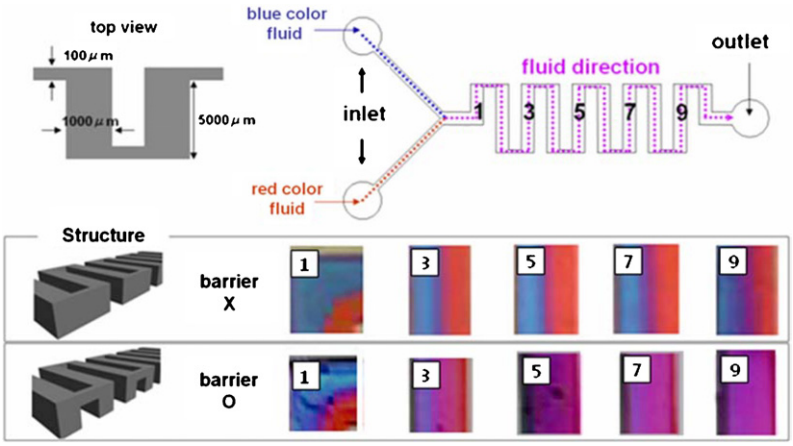


**Figure 8.** Experimental method and images of the mixing chamber in the square type device with and without mixers.

in series was placed over the liquid PDMS film, the height of the meniscus in the wide channel was lower than that in the narrow one [14].

This phenomenon makes it possible to build a barrier structure in the microchannel without aligning the two layers. The conventional method for a 3D structure needs 2 PDMS layers of different depths that also need to be aligned before bonding. Oxygen plasma bonding of PDMS with alignment entails tedious work with much caution and limited time due to the rapid deterioration of the active oxygenated surface. Therefore, the suggested method eliminates the complex fabrication process and saves time and labor. The process flow is presented in figure 7(*b*). First, the SU-8 mold for the microchannel (channel layer) was fabricated and PDMS was poured on it, followed by curing. After separating the solidified PDMS layer from the SU-8 mold, the channel layer was put on the liquid PDMS film, which was coated on a supporting layer. Then, the varying capillary height formed a barrier structure between the narrow and wide channels due to surface tension. After curing and separation, we could create a continuous structure with barriers.

The widths of the narrow and wide channels were 100 $\mu$m and 1000 $\mu$m, respectively. The thickness of the liquid PDMS film was coated for 1 min at 4000 rpm in the spin-coater, and the channel layer on the substrate was cured under a 50 g load. The cross-sections of the fabricated device with a straight channel were inspected to observe the effect formed by the surface tension as given in figure 7(*a*). The rising height in the wide channel was not clearly seen, but the height in the narrow channel was about 365 $\mu$m. The difference in depth between the two channels proved that the barrier structure was constructed in the microchannel with a variation of channel width.

### *3.2. Effect of the barrier structure in micro mixers*

To investigate the effect of the barrier on mixing, two fluids were injected in straight channels with a barrier and no barrier. Blue dye and red dye were dissolved in 99% ethyl alcohol and were injected into each inlet. The serpentine mixer with no barrier presented inefficient mixing even at subsection 9 as shown in figure 8. However, the mixer with barriers showed the two fluids were merged from subsection 3 and almost completely mixed in subsection 7. The barrier structure fabricated by surface tension dramatically improved mixing efficiency especially in the serpentine channel.

The 3D flows of mixers obtained from simulation (CFD-RC) can explain the efficient mixing of barrier structures. Figure 9 shows the mixing of two fluids at the vertical cross-section and the velocity vectors at the middle horizontal plane. When the two fluids turn around at the first corner, secondary flow rotates the fluids. When the barrier was not formed, the rotated fluid restores the original separated flow at the next corner since the fluids just followed the stream line of the laminar flow. However, the barrier structure induces a vortex at the outlet of the barrier and chaotic flow as reported by Simonnet [18]. When the fluids moved from the narrow channel into the wide channel, the vortex of fluids was observed in the wide channel in figure 9(*b*).

### *3.3. Characterization of the 3D serpentine mixer*

The mixing efficiency was quantitatively evaluated by the change of the pH indicator color. 0.1 M solution of phenolphthalein and sodium hydroxide (NaOH) dissolved in 99% ethyl alcohol was used to characterize the mixing performance of the serpentine mixer with the barrier. The images in the eight subsections were extracted with 9 by 9 pixels as shown in figure 10(*a*). Those were converted into a grayscale image and the intensity data of 81 pixels were obtained numerically using Matlab. The numerical data range from 0 to 255, where zero is white and 255 is black. The average intensity of each image is the degree of mixing, which is calculated by [7]

$$\bar{I} = \sum_{i=1}^{N} I_i, \tag{4}$$

where $I_i$ is the intensity of one pixel, and $N$ is the total number of pixels in the subsection image.

The normalized average intensity is plotted as a function of the Reynolds number ($Re$) in figure 10(*b*), when the flow rate ranges from 0.14 mL min$^{-1}$ to 1.25 mL min$^{-1}$. In the

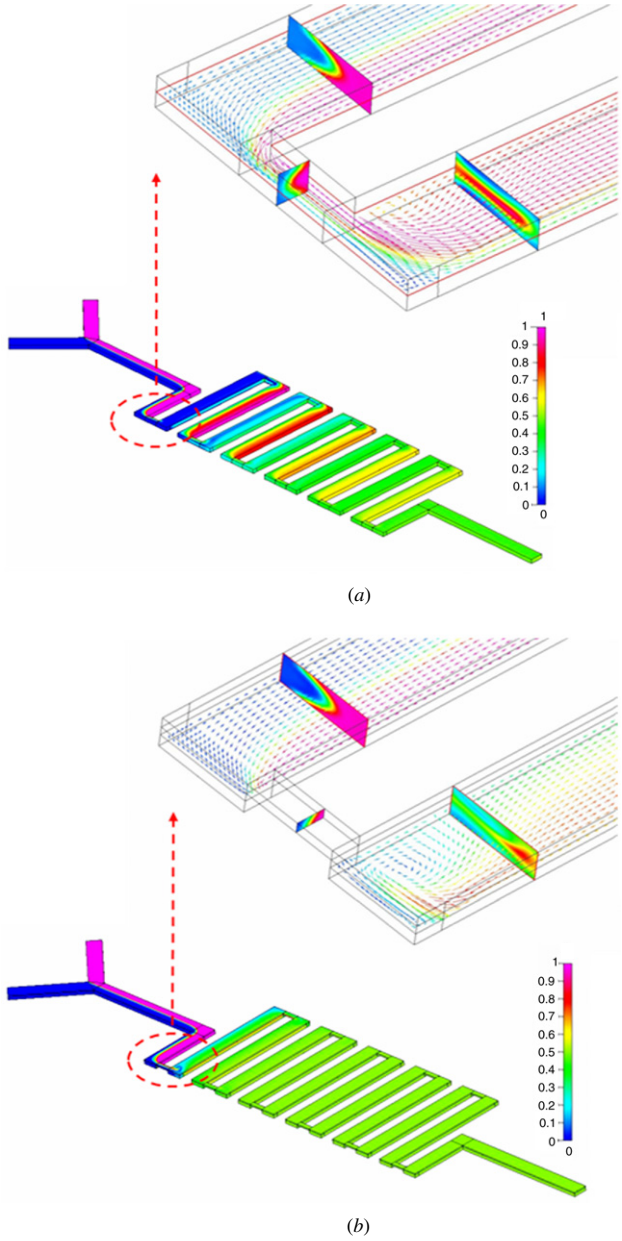


**Figure 9.** Simulation results performed in CFD-RC. (*a*) Micro mixer without barriers and (*b*) micro mixer with barriers.

region of $Re < 10$, two fluids are fully mixed regardless of the structure since the diffusion of ions is fast enough to mix while flowing through the channel. However, at a range of $Re > 10$, the fast flow does not allow enough time for the ions to diffuse and the device without a barrier shows that the fluids were not fully mixed. It has a normalized average intensity of 0.7, while the barrier mixer has a normalized average intensity from 0.8 to 0.9, where $Re$ is between 10 and 50. Hence, the barrier serpentine mixer demonstrates more efficient mixing than the device without a barrier. As fluid flows faster ($50 < Re < 100$), the secondary flow with axial flow produces a chaotic advection [19–22], which increases the interfacial area and leads to rapid mixing.

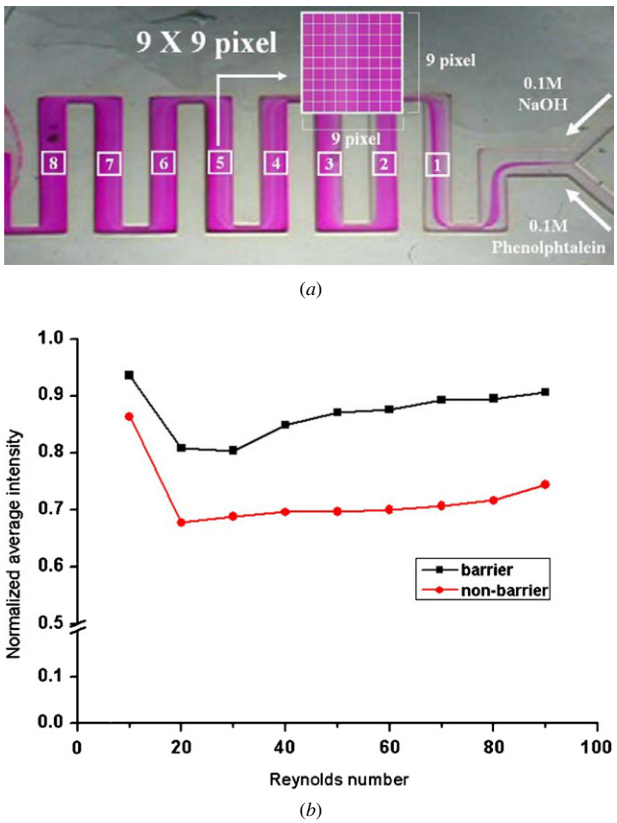


**Figure 10.** Experimental method and images of the mixing chambers of the square wave type mixer. (*a*) Method of analyzing mixing between Phenolphtalein and NaOH and (*b*) graph of normalized average intensity in the final chamber of a device with and without a barrier structure.

## 4. Conclusion

A novel fabrication method enables the fabrication of a round channel using the surface tension of PDMS. It is simple, convenient and advantageous with an easy bonding process without any chemical treatment. The shape of the cross-section could be modified by the load pressure and the contact area to fabricate a U shape, semi-circle, ellipse and circle. Furthermore, we could easily create a micro mixer with barriers using only one mask without alignment, because the capillary height depends on the channel width. The fabricated 3D serpentine mixer was tested at a range of Reynolds numbers from 10 to 90. As expected from the simulation, the 3D serpentine mixer was more effective than the planar serpentine channel. It was caused by the enhanced vortex and chaotic flow induced by the stirring effect in the barrier.

This fabrication method will be useful in very subtle applications such as the separation of samples, since round corners of the channel could minimize clogging and loss of samples at the corners of the channel. The channel made by surface tension is also appropriate to make a PDMS membrane valve owing to the membrane's round deformation. Although the effect of load pressure and contact area were discussed as process parameters in creating various channel shapes, more parameters need to be studied to minimize the variations in fabrication such as temperature, viscosity of the PDMS and initial thickness of the liquid PDMS. The relation between

the squeezed thickness and the load pressure also needs to be analyzed for exact control of the rising height.

## Acknowledgments

This research has been supported by the Intelligent Microsystem Center (IMC; http://www.microsystem.re.kr), which carries out one of the 21st century's Frontier R&D Projects sponsored by the Korea Ministry of Commerce, Industry and Energy.

## References

[1] Duffy D C, McDonald J C, Schueller O J A and Whitesides G M 1998 Rapid prototyping of microfluidic systems in poly(dimethylsiloxane) *Anal. Chem.* **70** 4974–84

[2] McDonald J C, Chabinyc M L, Metallo S J, Anderson J R, Stroock A D and Whitesides G M 2002 Poly(dimethylsiloxane) as a material for fabricating microfluidic devices *Acc. Chem. Res.* **74** 491–9

[3] Chen C, Hirdes D and Folch A 2003 Gray-scale photolithography using microfluidic photomasks *Proc. Natl Acad. Sci.* **100** 1499–504

[4] Futai N, Gu W and Takayama S 2004 rapid prototyping of microstructures with bell-shaped cross-sections and its application to deformation-based microfluidic valves *Adv. Mater.* **15** 1320–3

[5] Unger M A, Chou H P, Thorsen T, Scherer A and Quake S R 2003 *Science* **288** 113

[6] Gerhart P M 1992 *Fundamentals of Fluid Mechanics* 2nd edn (Reading, MA: Addison-Wesley)

[7] Liu R H, Stremler M A, Sharp K V, Olsen M G, Santiago J G, Adrian R J, Aref H and Beebe D J 2000 *J. Microelectromech. Syst.* **9** 190–7

[8] Wu H, Huang B and Zare N 2005 Construction of microfluidic chips using polydimethylsiloxane for adhesive bonding *Lab Chip* **5** 1393–8

[9] Satyanarayana S, Karnik R N and Majumdar A 2005 Stamp and stick room temperature bonding technique for microdevices *J. Microelectromech. Syst.* **14** 392–9

[10] Hong C C, Choi J W and Ahn C H 2004 A novel in-plane passive microfluidic mixer with modified Tesla structures *Lab Chip* **4** 109–13

[11] Jen C P, Wu C Y, Lin Y C and Wu C Y 2003 Design and simulation of the micromixer with chaotic advection in twisted microchannels *Lab Chip* **3** 77–81

[12] Hessel V, Lowe H and Schönfeld F 2004 Micromixers—a review on passive and active mixing principles *Chem. Eng. Sci.* **60** 2479–501

[13] Suh K Y, Chu S W and Lee H H 2004 W-shaped meniscus from thin polymer films in microchannels *J. Micromech. Microeng.* **14** 1185–9

[14] Y Suh K, Kim S and Lee H H 2001 Capillary force lithography *Adv. Mater.* **13** 1386–7

[15] Lee K S, Kim C, Kim Y H, Lee J W, Kang J Y, Oh M H, Ju B K and Lee S K 2005 Fabrication of rounded cross-sectional microchannel using surface tension of PDMS *Transducers* **2** 1505–8

[16] Gennes P D, Brochard-Wyart F and Quere D 2004 *Capillarity and Wetting Phenomena* (Berlin: Springer)

[17] Bao M, Yang H, Sun Y and French P J 2003 Modified Reynolds' equation and analytical analysis of squeeze-film air damping of perforated structures *J. Micromech. Microeng.* **13** 795–800

[18] Simonnet C and Groisman A 2005 Chaotic mixing in a steady flow in a microchannel, *Phys. Rev. Lett.* **94** 134501–4

[19] Kim D S, Lee S W, Kwon T H and Lee S S 2004 A barrier embedded chaotic micromixer *J. Micromech. Microeng* **14** 798–05

[20] Howell P B, Mott A R, Fertig S, Kaplanc C R, Golden J P, Oran L S and Ligler F S 2005 A microfluidic mixer with grooves placed on the top and bottom of the channel *Lab Chip* **5** 524–30

[21] Stroock A D, Dertinger S K W, Ajdari A, Mezic I, Stone H A and Whitesides G M 2002 Chaotic mixer for microchannels *Science* **295** 647–51

[22] Squires T M and Quake S R 2005 Microfluidics: fluid physics at the nanoliter scale *Rev. Mod. Phys.* **77** 977